European Polymer Journal 45 (2009) 2434–2442

Contents lists available at ScienceDirect

European Polymer Journal

journal homepage: www.elsevier.com/locate/europolj

Phase separation and phase dissolution in poly(ε-caprolactone)/poly(styrene-co-acrylonitrile) blend

Petr Svoboda [a,*], Dagmar Svobodova [a], Petr Slobodian [a], Dagmar Merinska [a], Yukiko Iizuka [b], Toshiaki Ougizawa [b], Takashi Inoue [c]

[a] Faculty of Technology, Tomas Bata University in Zlin, nam. TGM 275, 762 72 Zlin, Czech Republic
[b] Department of Organic and Polymeric Materials, Tokyo Institute of Technology, 2-12-1-S8-33, Ookayama, Meguro-ku, Tokyo 152-8552, Japan
[c] Department of Polymer Science and Engineering, Yamagata University, Yonezawa 992-8510, Japan

ARTICLE INFO

Article history:
Received 24 November 2008
Received in revised form 17 April 2009
Accepted 22 April 2009
Available online 3 May 2009

Keywords:
Spinodal decomposition
Phase dissolution
Polymer blends
PCL
SAN

ABSTRACT

A blend of poly(ε-caprolactone) (PCL) and poly(styrene-co-acrylonitrile) (SAN) containing 27.5 wt% of acrylonitrile having the critical composition (80/20 PCL/SAN) was studied. This PCL/SAN blend having a lower critical solution temperature (LCST) phase boundary at 122 °C offered an excellent opportunity to investigate, firstly the kinetics of phase separation above LCST (125–180 °C), and secondly the kinetics of phase dissolution below LCST (50–115 °C). The blend underwent a temperature-jump above LCST where spinodal decomposition (SD) proceeded, yielding a regularly phase-separated structure (SD structure). Then, it was quenched to the temperatures below LCST when the phase dissolution proceeded. Optical microscopy was used to observe the spinodal decomposition qualitatively while light scattering was used to characterize the phase separation and phase dissolution quantitatively. It was found that during phase dissolution the peak maximum moved towards a smaller angle (wavelength of concentration fluctuations increased) while the peak intensity decreased. This behavior was explained by a model. Also it was found that the fastest phase dissolution kinetics at 80 °C, which was characterized by an apparent diffusion coefficient, was about 10 times slower than the kinetics of phase separation at 180 °C.

1. Introduction

Poly(ε-caprolactone) (PCL) is a linear semicrystalline aliphatic polyester that became available commercially following efforts at Union Carbide to identify synthetic polymers that could be degraded by microorganisms. The high solubility of PCL, its low melting point (59–64 °C), and its exceptional ability to form blends has stimulated research on its application as a biomaterial. PCL degrades at a slower pace than PLA (polylactic acid) and can therefore be used in drug delivery devices that remain active for over 1 year [1].

Industrially produced copolymer of styrene and acrylonitrile (SAN) usually contains 15–35 wt% of acrylonitrile and is prepared by radical polymerization. The higher the acrylonitrile content, the greater the heat and chemical resistance, impact strength, toughness, scratch resistance and barrier properties. SAN is frequently used in households as well as in industry.

Quite many scientists have studied PCL/SAN blends, several examples are listed here [2–17]. PCL and SAN are miscible only when SAN contains 8–28 wt% of acrylonitrile. Near the boarders of this "miscibility window", the lower critical solution temperature (LCST) behavior was observed. In this study SAN with 27.5 wt% of acrylonitrile (AN) was used.

Being driven by thermal noises, local concentration in a polymer blend fluctuates continually. When temperature

* Corresponding author. Tel.: +420 576 031 335; fax: +420 577 210 172.
E-mail address: svoboda@ft.utb.cz (P. Svoboda).

0014-3057/$ - see front matter © 2009 Elsevier Ltd. All rights reserved.
doi:10.1016/j.eurpolymj.2009.04.027

is changed, the distribution of wavelength of concentration fluctuations changes until it reaches a new equilibrium. If a temperature change exceeds a certain limit, concentration fluctuations grow enormously and the blend undergoes phase separation through spinodal decomposition (SD) mechanism. Dynamics of fluctuation growth during SD has been extensively investigated in the last decades because of its theoretical as well as practical importance, e.g. by Hashimoto et al. [18–22].

When the temperature of a blend undergoing SD is changed to a value in the single-phase region, concentration fluctuations that had grown at one time in the spinodal region, gradually attenuate. Dynamics of such attenuation of concentration fluctuations is expected to follow the same mechanism as the growth of fluctuations during SD [23]. However, only a few experiments have been made to investigate the dynamics of attenuation of concentration fluctuations [23–29], which makes a marked contrast with the number of experimental studies performed to clarify the dynamics of fluctuation growth during the phase separation. Therefore, our research focused on this not so thoroughly understood field.

In this study PCL/SAN-27.5 blend exhibiting LCST behavior with critical composition (80/20) was investigated. Firstly the blend underwent phase separation at various temperatures above LCST giving us an opportunity to study the spinodal decomposition by optical microscopy and time-resolved light scattering (TRLS). Then the phase-separated blend was quenched to various temperatures below LCST where we could study the process of phase dissolution. Dynamics of attenuation of concentration fluctuations was experimentally investigated by light scattering.

2. Experimental

The PCL was a commercial polymer of Union Carbide Co. (PCL-767; $M_w = 40{,}400\ \mathrm{g\ mol^{-1}}$, $M_w/M_n = 2.61$). SAN containing 27.5 wt% of acrylonitrile (SAN-27.5) was synthesized at 60 °C using ethylbenzene as a solvent and azoisobutyronitrile (AIBN) at a concentration of 0.02 mol/l as an initiator; $M_w = 169{,}000\ \mathrm{g\ mol^{-1}}$, $M_w/M_n = 2.09$.

The solution cast method was used to prepare PCL/SAN blends with various compositions. PCL and SAN-27.5 were dissolved at 5 wt% of total polymer in 1,2-dichloroethane. The solution was cast onto a cover glass and the solvent was allowed to evaporate for 24 h at a room temperature. The dried film was annealed at 80 °C (below LCST that is at around 122 °C) for 1 min to achieve a single-phase state, and then it was subjected to a temperature jump to 125–180 °C (>LCST) to allow isothermal SD for the desired time (3–240 min). The decomposed sample was subjected to a temperature drop to temperatures below LCST (50–115 °C) where it was isothermally annealed to observe the phase dissolution.

For the optical microscopy observations, the specimen was initially annealed on first hot stage at desired temperature. The melted specimen was then placed onto a LINKAM hot stage of the microscope. Structural development during the isothermal annealing was observed under both the optical and the polarizing microscope (Olympus BH-2) equipped with a video recording system and exposure control unit (Olympus PM-20).

Real time analyses of the structure developments above and below LCST were carried out by light scattering method. A polarized He–Ne gas laser of 632.8 nm wavelength was applied vertically to the film specimen. The scattered light passed through an analyzer and then onto a highly sensitive CCD camera with 567 × 382 pixels in a sensor of dimension 13.3 × 8.8 mm (Princeton Instruments, Inc.). This allowed the time-resolved measurement of a one-dimensional angular distribution of scattered light with 576 points in a time scale of 0.14 s. The input data from the CCD camera was digitized by a ST-13X controller. The digitized data was stored in a personal computer equipped with Dyna-100 software for further analysis. Only V_v optical geometry was used, when the optical axis of the analyzer was set parallel to that of the polarizer.

3. Results and discussion

Fig. 1 shows the phase diagram of PCL/SAN-27.5 blend. All specimens of PCL/SAN-27.5 blends were optically clear, and no structure was observed by the microscope at 80 °C (above the melting temperature of PCL). When the specimens were heated above LCST, they became opaque, and a two-phase structure was observed.

As described in the experimental section, the blend was first annealed below LCST in one-phase region (point A). Then the sample was transferred onto another hot stage to various temperatures set above LCST (point B) and annealed isothermally there. Phase separation proceeded to various levels depending on temperature and duration of annealing at the point B. Finally, the phase-separated sample was quenched to various phase dissolution temperatures (50–115 °C) below LCST (point C).

In Fig. 2, the structural development in 80/20 PCL/SAN-27.5 after the temperature jump from 80 to 130 °C is shown. Initially no structure was seen. After 5 min, a

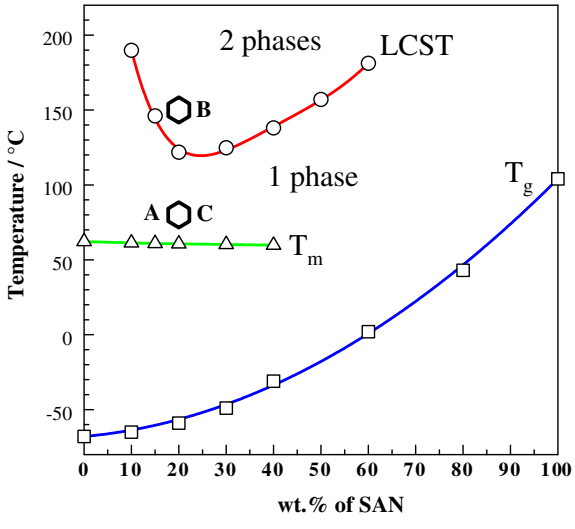

Fig. 1. Phase diagram of PCL/SAN-27.5 blend taken from our previous work [30].

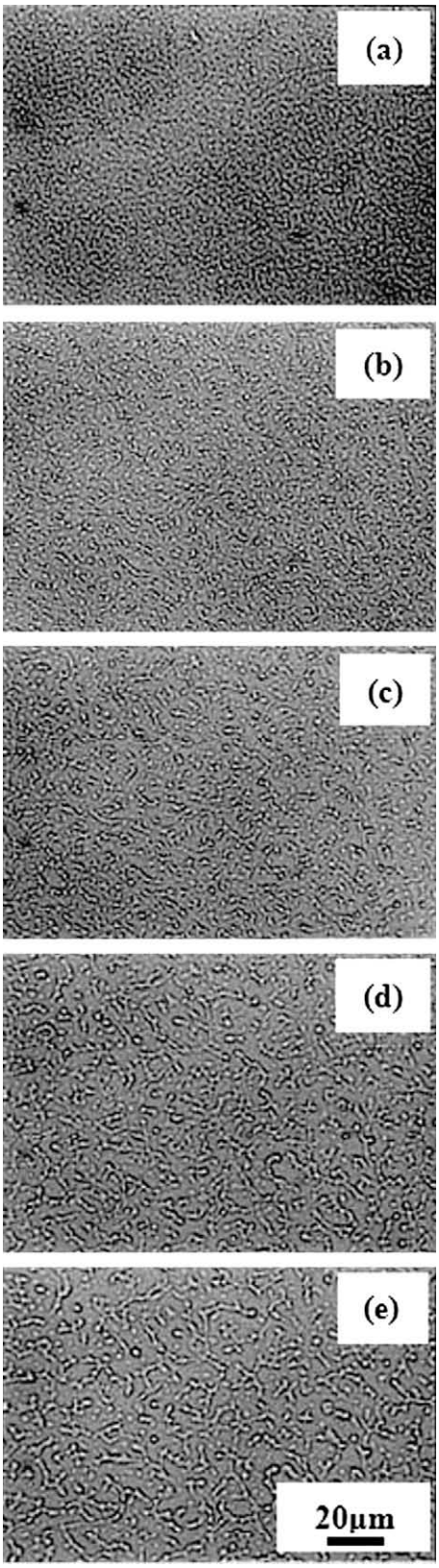

Fig. 2. Optical micrographs of PCL/SAN-27.5 (80/20) blend showing phase separation at constant temperature 130 °C developing in time: (a) 5 min, (b) 30 min, (c) 60 min, (d) 90 min, and (e) 120 min.

two-phase structure with a unique periodicity and phase connectivity was detected. The contrast of the structure became higher with the time of annealing (30 min). Then the structure became coarser and larger with time (60, 90, and 120 min).

Fig. 3 shows a typical example of the change in the scattering profile with annealing (demixing) time t at 130 °C. Here, the scattered light intensity I_{Vv} is shown as a function of the scattering vector q, given by [18]

$$q = \frac{4\pi}{\lambda} \sin\left(\frac{\theta}{2}\right) \tag{1}$$

where λ is the wavelength of the light in the specimen and θ is the scattering angle. At t = 0 min the scattering intensity is very weak and the profile has hardly any angle dependence, suggesting a homogeneous mixture. The homogeneous mixture starts to phase separate by annealing at 130 °C, as shown by the increase in the scattering intensity. The existence of a scattering peak that is moving to lower values of angle suggests that demixing proceeds by spinodal decomposition (SD) mechanism.

The SD process in *near-critical* mixtures can be divided into (i) early stage, (ii) intermediate stage, and (iii) late

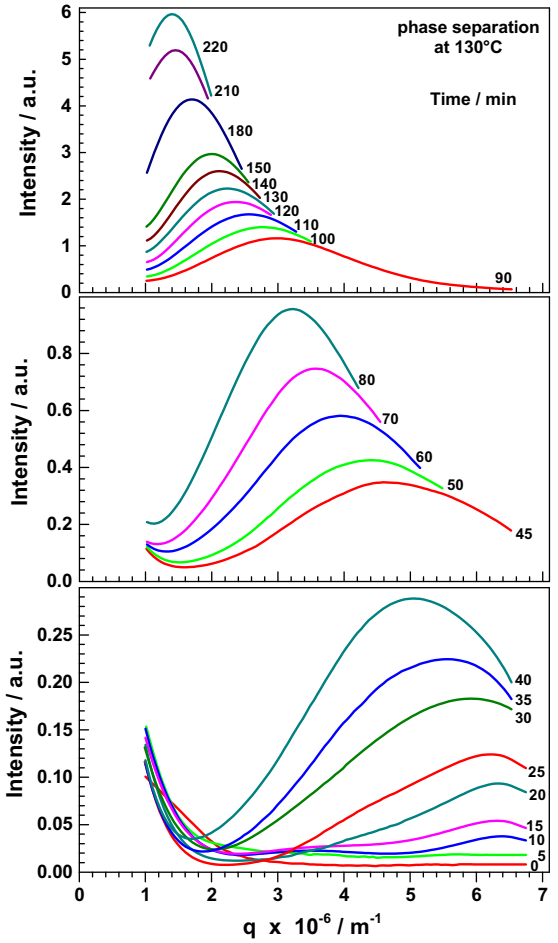

Fig. 3. Change of light-scattering V_v profile of PCL/SAN-27.5 (80/20) blend during isothermal phase separation at 130 °C.

stage [31]. In the early stage the time evolution of the concentration fluctuations can be approximated by the linearized theory, first proposed by Cahn [32]. The characteristic wavenumber $q_m(t,T)$, which is related to the domain spacing $\Lambda_m(t,T)$,

$$\Lambda_m(t) = \frac{2\pi}{q_m(t)} \tag{2}$$

of the dominant mode of the concentration fluctuations at time t and phase-separation temperature T is independent of t. The intensity of the Fourier mode of the fluctuations with wavenumber q, $I(q,t,T)$, grows exponentially with the time. The intermediate stage is characterized by a decrease of $q_m(t,T)$ as well as a further increase of the intensity due to a nonlinear nature in the time evolution of the concentration fluctuations. In the late stage the two phases reach equilibrium composition and the interface between the two phases narrows to equilibrium thickness. The domains, however, $\Lambda_m(t,T)$ are still increasing in order to lower the interfacial free energy of the system [31].

In order to observe the whole process of SD it is convenient to plot the position of the maximum q_m and intensity at the maximum I_m (from Fig. 3) as a function of time in a double logarithmic plot, see Fig. 4. In this way one is able to divide the SD process into three stages. In the early stage the position of the maximum q_m stays almost constant. Then in the intermediate and late stages a scaling analysis is being used. Binder and Stauffer [33] proposed scaling rules, assuming that clusters aggregate by a diffusion process and coalesce into larger clusters and described the self-similar growth of the structure by the time evolution of $q_m(t,T)$ and $I_m(t,T)$ as

$$q_m(t,T) \sim t^{-\alpha} \tag{3}$$

and

$$I_m(t,T) \sim t^{\beta} \tag{4}$$

Various models and various α and β exponents were also reported, e.g. by Langer et al. [34] or Siggia [35]. In the intermediate stage a relation $\beta > 3\alpha$ is observed. The late stage is reached when $\beta = 3\alpha$ [31,36–40]. In the late stage the two phases attain equilibrium compositions, and self-similar growth of the structure can be observed. Summary of the analysis presented in Fig. 4:

(1) In the **early stage**, there is no increase in wavelength Λ_m, (q_m stays constant) concentration fluctuations $\Delta\phi(t)$ (ϕ is volume concentration) are increasing and the slope of the line (α) is 0. The duration for our case was found 0–25 min. This is in agreement with observation by optical microscopy (see Figs. 2a and b) when there is only very small increase in the wavelength Λ_m between 5 and 30 min.
(2) In the **intermediate stage**, both the amplitude of the concentration fluctuations $\Delta\phi(t)$ and wavelength $\Lambda_m(t)$ of the fluctuations grow with time, and the position of maximum q_m in Fig. 3 is decreasing to lower angles, the slope of the line α is gradually increasing. Because β is almost a constant, β/α is gradually decreasing until it reaches value 3. The duration was found to be 25–70 min.
(3) In the **late stage**, where the value $\Delta\phi$ reaches an equilibrium value $\Delta\phi_e$ determined by the coexistence curve and the phase-separation temperature (in Fig. 1), only Λ_m grows with time. The duration of the late stage was 70–220 min and the ratio $\beta/\alpha = 3$.

The variation of Λ_m in time for PCL/SAN-27.5 (80/20) blends at two different temperatures 130 and 150 °C is plotted in Fig. 5. The values of Λ_m can be used for designing the desired size of domains. And indeed we used this plot to prepare two different samples with apparently the same wavelength of the concentration fluctuations Λ_m being about 4.3 μm, the first one prepared by spinodal decomposition at 130 °C for 220 min and the other at 150 °C for

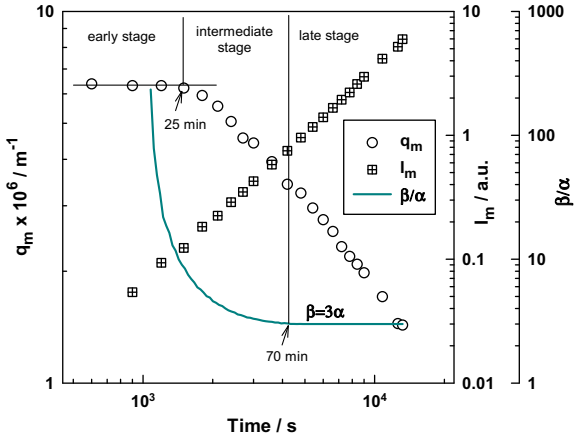

Fig. 4. Time evolution of the characteristic wavenumber at maximum q_m, intensity at maximum I_m and β/α ratio for PCL/SAN-27.5 (80/20) blend during isothermal phase separation at 130 °C.

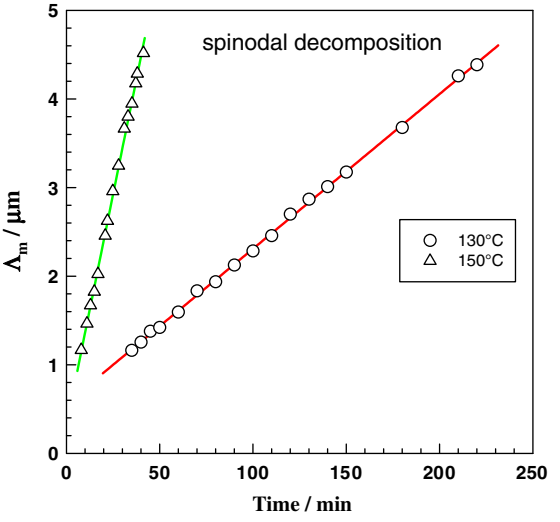

Fig. 5. Wavelength of concentration fluctuations Λ_m (from V_v scattering) vs. time for PCL/SAN-27.5 (80/20) blend. Samples were heated to 80 °C for 1 min (one-phase region) and then transferred to another hot stage at 130 °C or 150 °C (two-phase region).

38 min. These two supposedly same samples were then subjected to phase dissolution (PD) at 90 °C.

The results are shown in Figs. 6 and 7. The light scattering machine was set to measure precisely the intensity at smaller angles (compared to Fig. 3). At first please note that the initial peak at 0 min is a little broader in the case of the sample phase separated at 150 °C compared to that separated at 130 °C. This indicates quite narrow particle size distribution of the phase-separated structure created at 130 °C and a coexistence of larger and smaller particles created at 150 °C.

In both cases, the light scattering peak is decreasing and the position of the maximum is shifting towards the lower angle. There are several possible interpretations of the shift of the peak maximum in Figs. 6 and 7, one of which is the faster decay of the high-q Fourier components in the concentration pattern. Only the slower components with long wavelengths (small q) survive at longer times. This results in an effective peak shift towards small q (small angles) during the dissolution process.

This is schematically shown in Fig. 8, particles No. 1 and 2. While the large particle No. 1 survives up to Fig. 8c particle No. 2 is in Fig. 8c already dissolved. Light scattering at late stage of phase dissolution detects only the remaining particle No. 1. Another possible interpretation of the peak shift towards smaller angle is coalescence of close particles No. 3 and 4. The actual growth of the particles during phase dissolution is possible too, as it was observed directly by TEM by Okada [22,23] and calculated by using a model by Cheng [26]. This is schematically shown by particle No. 5. In our particular PCL/SAN (80/20) system the particles are formed by SAN-rich phase. SAN has rather high T_g (about 103 °C) while for PCL $T_g = -66$ °C and $T_m \cong 60$ °C. Also molecular weight of SAN (M_w = 169,000 g mol^{-1}) is higher compared to PCL (M_w = 40,400 g mol^{-1}). Above mentioned facts might contribute to much higher mobility of PCL compared to SAN at phase

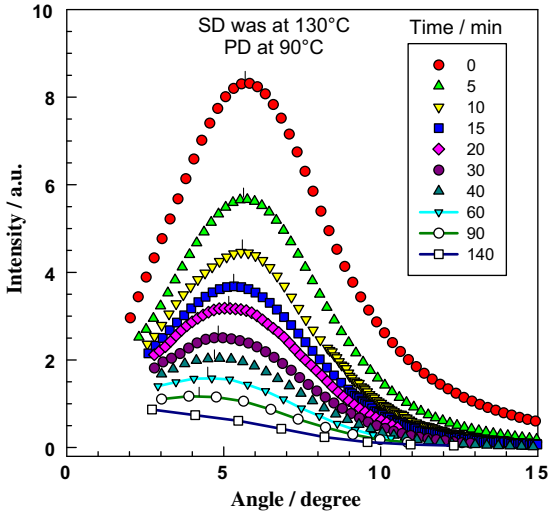

Fig. 6. Change of light scattering profile of PCL/SAN-27.5 (80/20) blend during isothermal phase dissolution at 90 °C after phase separation at 130 °C for 220 min.

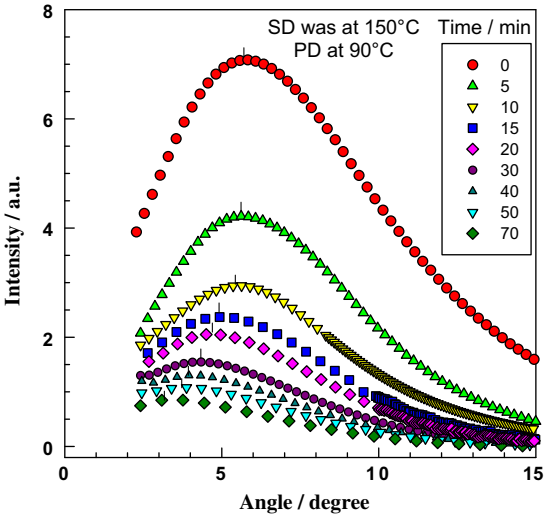

Fig. 7. Change of light scattering profile of PCL/SAN-27.5 (80/20) blend during isothermal phase dissolution at 90 °C after phase separation at 150 °C for 38 min.

dissolution temperature (90 °C). Thus it is possible that PCL molecules diffuse into SAN particle faster than SAN molecules are leaving. This would result in swelling of SAN particles.

Concerning **phase separation**: the existence of scattering peak that is moving to lower values of scattering angle (already shown Fig. 3) indicates that the demixing proceeds by the spinodal decomposition (SD) mechanism. To confirm this point, we analyzed the early stage on the basis of the linearized Cahn–Hilliard theory [32,41].

Cahn in 1965 [32] laid a basis for mathematical treatment of spinodal decomposition. He started with expression for free energy of inhomogeneous solution whose composition everywhere differs only slightly from the average composition, and with small composition gradients.

$$F = \int [f(c) + \kappa(\nabla c)^2] dV \tag{5}$$

Here $f(c)$ is the free-energy density of homogeneous material of composition c, $\kappa(\nabla c)^2$ is the additional free-energy density if the material is in a gradient in composition. In the development of the theory it became convenient to consider the Fourier components of the composition rather than the composition. Because of the orthogonality of the Fourier components, ΔF is the sum of contributions from each Fourier component separately.

The kinetics of the initial stages of phase separation can be obtained by solving the diffusion equation. We define a mobility M which is (minus) the ratio of diffusional flux to the gradient in chemical potential

$$J_B = -J_A = M\nabla(\mu_A - \mu_B) \tag{6}$$

Simple thermodynamic considerations show that M must be positive if diffusion which results spontaneously from the chemical potential gradient is to result in a decrease in free energy. We obtain $\mu_A - \mu_B$ from the variational derivative of F in Eq. (5),

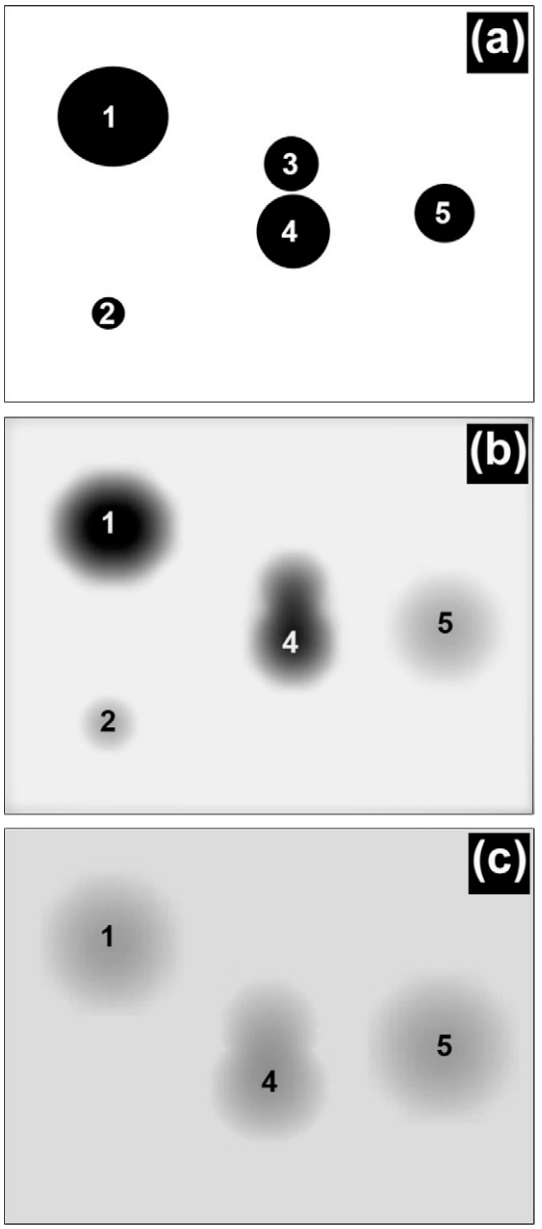

Fig. 8. Model of phase dissolution development in time derived from light scattering data shown in Figs. 6 and 7.

$$\mu_A - \mu_B = \left(\frac{\delta F}{\delta c_A}\right) = \left(\frac{\partial f}{\partial c_A}\right) - 2\kappa\nabla^2 c_A + \text{terms higher in order and degree} \tag{7}$$

We may discard the higher order terms if we are only interested in the initial stages. By substituting Eq. (7) into Eq. (6) and taking the divergence, and keeping only first degree terms, we obtain the following diffusion equation:

$$\frac{\partial c}{\partial t} = M\left(\frac{\partial^2 f}{\partial c^2}\right)\nabla^2 c - 2M\kappa\nabla^4 c \tag{8}$$

Since the coefficient of $\nabla^2 c$ may be identified with a diffusion coefficient we see that at the spinodal the diffusion coefficient changes sign. The solution to Eq. (8) is

$$c - c_0 = e^{[R(\beta)t]}\cos(\beta\mathbf{r}) \tag{9}$$

Where β is wavenumber and $R(\beta)$ is given by

$$R(\beta) = -M\left(\frac{\partial^2 f}{\partial c^2}\right)\beta^2 - 2M\kappa\beta^4 \tag{10}$$

Cahn has developed his model for small molecules in metallurgy. His equations were slightly modified for polymer blends. These days we are using g instead of f and q instead of β. Light scattering became popular in quantitative evaluation of spinodal decomposition in polymer blends. Here, in the initial stage of phase separation (or phase dissolution), the intensity of scattered light (I) is expected to increase (or decrease) exponentially with time t.

$$I_{Vv}(q,t) \propto e^{2R(q)t} \tag{11}$$

where $R(q)$ is the growth rate (or decay rate) of concentration fluctuation at the scattering vector q. Today $R(q)$ is given by (essentially the same as Eq. (10) in 1965)

$$R(q) = -Mq^2\left(\frac{\partial^2 g}{\partial c^2} + 2\kappa q^2\right) \tag{12}$$

where M is the mobility, g is the free-energy density of the blend with composition c, and κ is the gradient energy coefficient.

Cahn started with describing the Gibbs free energy of fluctuating system by a sum of the local free energy of mixing and the square of concentration gradient term. The gradient term remains in Eq. (12) as the second term. The first term of Eq. (12) is the second derivative of g which is the thermodynamic driving force for fluctuation growth (i.e., the degree of instability of homogeneously mixed state). The second term of Eq. (12) suggests that a very sharp gradient with large q (short wavelength of fluctuation)

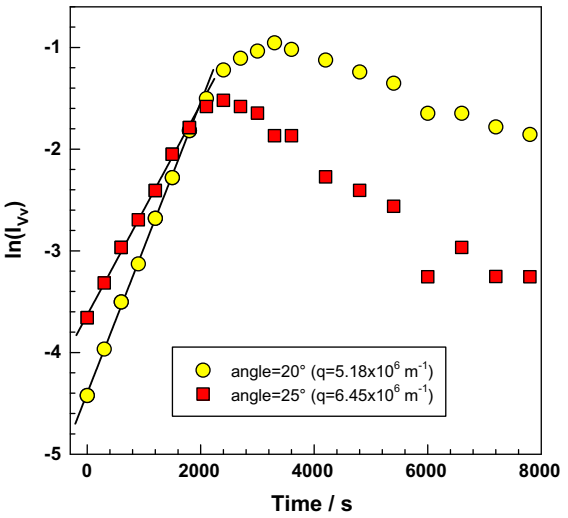

Fig. 9. Change of $\ln(I_{Vv})$ in time during spinodal decomposition at 130 °C (from light scattering). Evaluation of slopes for various angles.

suppresses the fluctuation growth. In contrast, the fluctuation with small q (long wavelength) grows slowly, because the molecules should diffuse long distance for the fluctuation growth. Then, there should exist a peak of rate constant $R(q)$ at a particular q.

As it was mentioned earlier and described by Eq. (11) in the early stage of spinodal decomposition the intensity should increase exponentially with time. This was indeed observed and is shown in Fig. 9. We used natural logarithm of intensity and therefore the plot yields straight lines in the initial stage. Then one can estimate the growth (or decay) rate $R(q)$ of concentration fluctuations from the initial slope of a $\ln(I_{Vv})$ vs. t plot (in Fig. 9 for phase separation and in Fig. 10 for phase dissolution) for different angles (or q values).

After such detailed analysis, it is possible to calculate the $R(q)/q^2$ vs. q^2 plot as it is shown in Fig. 11 for SD and Fig. 12 for PD for various temperatures. The apparent diffusion coefficient D_{app} is defined by

$$D_{app} = -M\left(\frac{\partial^2 g}{\partial c^2}\right) \tag{13}$$

and can be obtained from $R(q)/q^2$ vs. q^2 plot as the intercept of the $R(q)/q^2$ axis in Figs. 11 and 12.

The apparent diffusion coefficient D_{app} obtained in this way was positive for phase dissolution and negative for

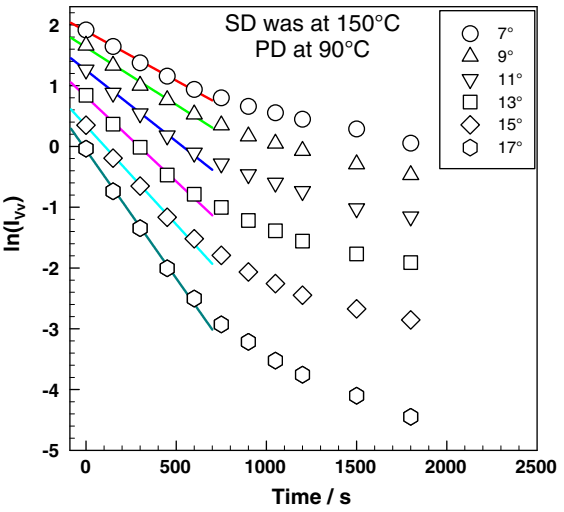

Fig. 10. Change of $\ln(I_{Vv})$ in time during phase dissolution at 90 °C (from light scattering). Evaluation of slopes for various angles.

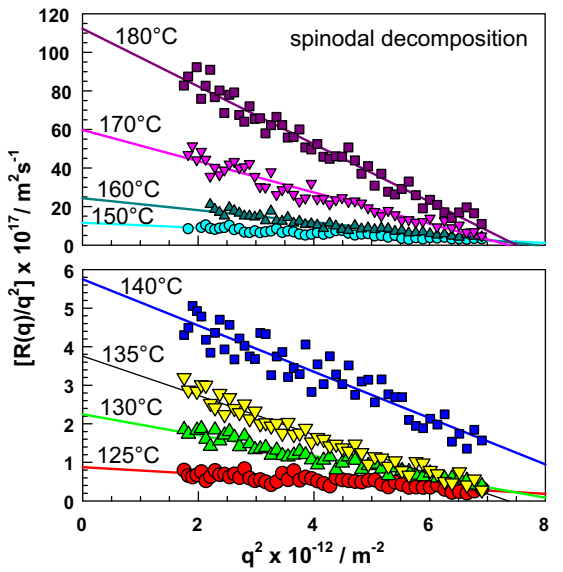

Fig. 11. Plot of $R(q)/q^2$ vs. q^2 of PCL/SAN-27.5 (80/20) blend: spinodal decomposition at 125–180 °C. $R(q)$ values were obtained by analysis of slopes shown by Fig. 9.

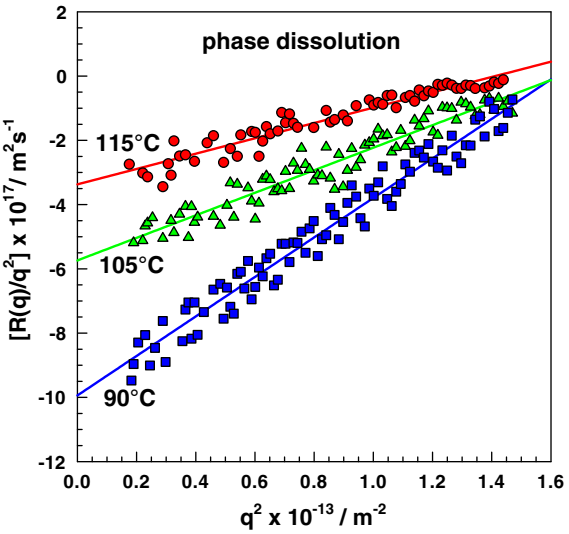

Fig. 12. Plot of $R(q)/q^2$ vs. q^2 of PCL/SAN-27.5 (80/20) blend: phase dissolution at 90, 105, and 115 °C after previous spinodal decomposition at 150 °C for 15 min. $R(q)$ values were obtained by analysis of slopes shown in Fig. 10.

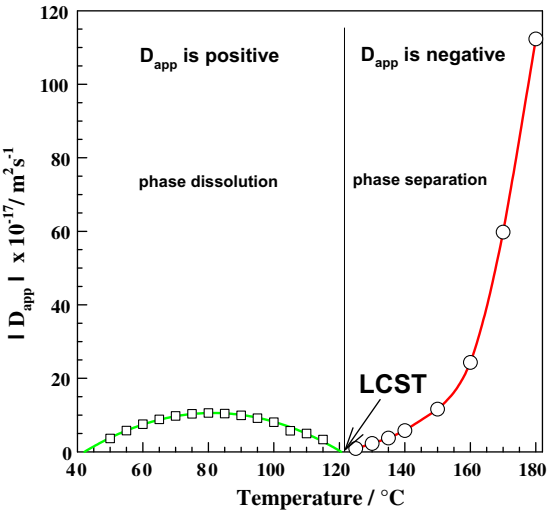

Fig. 13. Apparent diffusion coefficient for phase dissolution (squares) and phase separation (circles) as a function of annealing temperature. Lower critical solution temperature (LCST) is shown by arrow.

phase separation. It is interesting to compare the absolute values of D_{app} for SD and PD in one plot, see Fig. 13.

The D_{app} for phase dissolution was found to have values between 3 and 11 $\times$ 10^{-17} m^2 s^{-1} in the temperature range 50–115 °C. Closer to LCST the values are decreasing and in range 50–65 °C they are low as well. The diffusion should be slower at lower temperature due to a lower mobility. In our case, also the presence of a virtual upper critical solution temperature (UCST) around 40 °C, found earlier for similar systems [42], should cause the decrease in D_{app}. Comparable values of D_{app} for phase separation (just with opposite sign – negative values) were found in the temperature range 125–150 °C. By a further increase of the temperature the spinodal decomposition proceeded much faster, an example being value of D_{app} at 180 °C which is more than 10 times higher than the fastest phase dissolution. From the exponential-like curve one could assume that this difference would be probably even much higher (such as 100× or even 1000×) if we increased the temperature to e.g. 200 or 220 °C.

4. Conclusion

PCL/SAN-27.5 blend gave us an excellent opportunity to investigate the phase dissolution kinetics and to add some experimental data (that are still quite rare) to this subject. Firstly, we focused on the phase separation above LCST (being at 122 °C), and studied it qualitatively by optical microscopy (at 130 °C), and then quantitatively by light scattering at various temperatures (125–180 °C). The spinodal decomposition mechanism of phase separation was confirmed by the detailed data analysis based on Cahn–Hilliard theory. Secondly, the phase-separated structure was quenched to various temperatures below LCST (50–115 °C) to study the phase dissolution. The phase dissolution was affected by the temperature of previously performed spinodal decomposition. Based on light scattering data, a model of phase dissolution mechanism was created. There are several possible interpretations of the shift of the peak maximum during phase dissolution, one of which is the faster decay of the high-q Fourier components in the concentration pattern. Only the slower components with long wavelengths (small q) survive at longer times. This results in an effective peak shift towards small q (small angles) during the dissolution process. Again, for the PD, we were able to use linearized theory to obtain an apparent diffusion coefficient D_{app}. Finally, the D_{app} values were compared for SD and PD with the result showing that the fastest PD was about 10 times slower than the fastest SD in measured temperature range.

Acknowledgement

This work has been supported by the Ministry of Education of the Czech Republic as a part of the Project No. VZ MSM 7088352102.

References

[1] Ratner BD, Hoffman AS, Schoen FJ, Lemons EJ. Biomaterials science. New York: Elsevier Academic Press; 2004.
[2] Madbouly SA, Abdou NY, Mansour AA. Isothermal crystallization kinetics of poly(ε-caprolactone) with tetramethyl polycarbonate and poly(styrene-co-acrylonitrile) blends using broadband dielectric spectroscopy. Macromol Chem Phys 2006;207(11):978–86.
[3] Kiersnowski A, Piglowski J. Polymer-layered silicate nanocomposites based on poly(ε-caprolactone). Eur Polym J 2004;40(6):1199–207.
[4] Men Y, Strobl G. Critical strains in poly(ε-caprolactone) and blends with poly(vinyl methyl ether) and poly(styrene-co-acrylonitrile). Macromolecules 2003;36(6):1889–98.
[5] Aoki Y, Arendt O. Melt rheology of poly(ε-caprolactone)/poly(styrene-co-acrylonitrile) blends. J Appl Polym Sci 2001;82(8):2037–41.
[6] Kim SW, Jo WH, Lee MS, Ko MB, Jho JY. Preparation of clay-dispersed poly(styrene-co-acrylonitrile) nanocomposites using poly(ε-caprolactone) as a compatibilizer. Polymer 2001;42(24):9837–42.
[7] Hong Z, Shaw MT, Weiss RA. Structure evolution and phase behavior of polymer blends under the influence of shear. Polymer 2000;41(15):5895–902.
[8] Keroack D, Zhao Y, Prud'homme RE. Molecular orientation in crystalline miscible blends. Polymer 1999;40(1):243–51.
[9] Wang Z, Wang X, Yu D, Jiang B. The formation of ring-banded spherulites of poly(ε-caprolactone) in its miscible mixtures with poly(styrene-co-acrylonitrile). Polymer 1997;38(23):5897–901.
[10] Oudhuis AACM, Thiewes HJ, van Hutten PF, ten Brinke G. A comparison between the morphology of semicrystalline polymer blends of poly(ε-caprolactone)/poly(vinyl methyl ether) and poly(ε-caprolactone)/(styrene-acrylonitrile). Polymer 1994;35(18):3936–42.
[11] Li W, Prud'homme RE. Orientation and miscibility of poly(ε-caprolactone)/poly(styrene-co-acrylonitrile) mixtures. Polymer 1994;35(15):3260–7.
[12] Gan PP, Paul DR, Padwa AR. Phase behaviour of blends of homopolymers with α-methylstyrene/acrylonitrile copolymers. Polymer 1994;35(7):1487–502.
[13] Janathanan V, Kressler J, Karasz FE, Macknight WJ. Intramolecular interactions in poly(styrene-co-acrylonitrile)/poly(ε-caprolactone) blends. J Polym Sci B Polym Phys 1993;31(8):1013–7.
[14] Kressler J, Kammer HW, Silvestre C, Di Pace E, Cimmino S, Martuscelli E. Crystallization kinetics in blends of poly-ε-caprolactone and poly(styrene-ran-acrylonitrile). Polym Networks Blends 1991;1(4):225–33.
[15] Shah VS, Keitz JD, Paul DR, Barlow JW. Miscible ternary blends containing polycarbonate, SAN, and aliphatic polyesters. J Appl Polym Sci 1986;32(3):3863–79.
[16] Chiu SC, Smith TG. Compatibility of poly(epsilon-caprolactone) (PCL) and poly(styrene-*co*-acrylonitrile) (SAN) blends – II. The influence of the AN content in SAN copolymer upon blend compatibility. J Appl Polym Sci 1984;29(5):1797–814.
[17] Schulze K, Kressler J, Kammer HW. Phase behaviour of poly(ε-caprolactone)/poly(styrene-ran-acrylonitrile) blends exhibiting both liquid–liquid unmixing and crystallization. Polymer 1993;34(17):3704–9.
[18] Hashimoto T, Tsukahara Y, Kawai H. Dynamic small-angle X-ray scattering studies on diffusion of macromolecules in bulk. 2. Principle and preliminary experimental results. Macromolecules 1981;14(3):708–15.
[19] Hashimoto T, Kumaki J, Kawai H. Time-resolved light scattering studies on kinetics of phase separation and phase dissolution of polymer blends. 1. Kinetics of phase separation of a binary mixture of polystyrene and poly(vinyl methyl ether). Macromolecules 1983;16(4):641–8.
[20] Inaba N, Sato K, Suzuki S, Hashimoto T. Morphology control of binary polymer mixtures by spinodal decomposition and crystallization. 1. Principle of method and preliminary results on PP/EPR. Macromolecules 1986;19(6):1690–5.
[21] Nakai A, Shiwaku T, Hasegawa H, Hashimoto T. Spinodal decomposition of polymer mixtures with a thermotropic liquid crystalline polymer as one component. Macromolecules 1986;19(12):3008–10.
[22] Inaba N, Yamada T, Suzuki S, Hashimoto T. Morphology control of binary polymer mixtures by spinodal decomposition and crystallization. 2. Further studies on polypropylene and ethylene–propylene random copolymers. Macromolecules 1988;21(2):407–14.
[23] Okada M, Tao J, Nose T. Attenuation of concentration fluctuations after a quench to a temperature in the single-phase region. Polymer 2002;43(2):329–35.

[24] Okada M, Tao J, Nose T. Dissolution of phase-separated domains after a jump to a temperature in the single-phase region. Polymer 2002;43(26):7429–32.
[25] Akcasu AZ, Bahar I, Erman B, Feng Y, Han CC. Theoretical and experimental study of dissolution of inhomogeneities formed during spinodal decomposition in polymer mixtures. J Chem Phys 1992;97(8):5782–93.
[26] Cheng MH, Nauman EB. Non-linear diffusion with concentration-driven flows in miscible systems. Polymer 2003;44(21):6707–12.
[27] Okamoto M, Shiomi K, Inoue T. LCST-type phase behaviour and structure development during melt processing in a polycarbonate/poly(styrene-co-acrylonitrile) blend. Polymer 1995;36(1):87–91.
[28] Sato T, Han CC. Dynamics of concentration fluctuation in a polymer blend on both sides of the phase boundary. J Chem Phys 1988;88(3):2057–65.
[29] Takagi Y, Ougizawa T, Inoue T. Phase dissolution in polymer blends. Kinetics of dissolution and related problems in rubber technology. Polymer 1987;28(1):103–8.
[30] Svoboda P, Svobodova D, Chiba T, Inoue T. Competition of phase dissolution and crystallization in poly(ε-caprolactone)/poly(styrene-co-acrylonitrile) blend. Eur Polym J 2008;44(2):329–41.
[31] Ribbe AE, Hashimoto T. Real space analysis of the structural evolution of a polymer blend via spinodal decomposition. Macromolecules 1997;30(14):3999–4009.
[32] Cahn JW. Phase separation by spinodal decomposition in isotropic systems. J Chem Phys 1965;42(1):93–9.
[33] Binder K, Stauffer D. Theory for the slowing down of the relaxation and spinodal decomposition of binary mixtures. Phys Rev Lett 1974;33(17):1006–9.
[34] Langer J, Baron M, Miller HD. New computational method in theory of spinodal decomposition. Phys Rev A 1975;11(4):1417–29.
[35] Siggia ED. Late stages of spinodal decomposition in binary mixtures. Phys Rev A 1979;20(2):595–605.
[36] Fujita H, Hashimoto T, Takenaka M. Time change in the maximum of scattering intensity during spinodal decomposition. Macromolecules 1989;22(12):4663–4.
[37] Hashimoto T, Izumitani T. Effect of a block copolymer on the kinetics of spinodal decomposition of polymer blends. 1. Nonuniversality in scaled characteristic quantities versus reduced time. Macromolecules 1993;26(14):3631–8.
[38] Izumitani T, Hashimoto T. Effect of a block copolymer on the kinetics of spinodal decomposition of polymer blends. 2. Scaled structure factor. Macromolecules 1994;27(7):1744–50.
[39] Takeno H, Iwata M, Takenaka M, Hashimoto T. Combined light scattering and laser scanning confocal microscopy studies of a polymer mixture involving a percolation-to-cluster transition. Macromolecules 2000;33(26):9657–65.
[40] Jinnai H, Hasegawa H, Hashimoto T, Han CC. Time-resolved small-angle neutron scattering in intermediate and late-stage spinodal decomposition of DPB/HPI blends. Macromolecules 1991;24(1):282–9.
[41] Cahn JW, Hilliard JE. Free energy of a nonuniform system. I. Interfacial free energy. J Chem Phys 1958;28(2):258–67.
[42] Svoboda P, Kressler J, Chiba T, Inoue T, Kammer HW. Light-scattering and TEM analyses of virtual upper critical solution temperature behaviour in PCL/SAN blends. Macromolecules 1994;27(5):1154–9.